Final report for the project# 2106ANQ, "Sixtron Advanced Materials/Quebec, Cananda

Optimizing the silane-free silicon carbon nitride (SiC_xN_y) antireflection coating

Moon Hee Kang, Dr. Ajeet Rohatgi, Dr. Abasifreke Ebong, Brian Rounsaville

Table of Contents

Introduction

Plasma enhanced chemical vapor deposition (PECVD) silicon nitride (SiN_x) films are widely used for commercial silicon solar cells. SiN_x films provide excellent surface passivation on the phosphorus doped emitters because of their high positive fixed charge density, which causes an inversion or accumulation layer in p-type or n-type Si under the SiN_x. The optimum refractive index of the AR coating layer for an encapsulated solar cell is about 2.4, which is achievable by using silicon rich SiN_x films. However, such films absorb significant short wavelengths photons and decrease the quantum efficiency. Glunz et. al. and Martin et al reported on PECVD silicon carbide (SiC_x) films for surface passivation of crystalline silicon. Surface recombination velocity (SRV) less than 30 cm/s at the SiC_x / Si interface have been reported. SiC_x films also have a high refractive index (more than 2.3), suggesting that SiC_x may be an improvement over PECVD deposited SiN_x. Deposition of SiN_x and SiC_x films typically require dangerous pyrophoric silane (SiH_4), which is a significant inhibiting factor in the cost reduction economies-of-scale strategies employed by silicon PV plants. To eliminate the need for storage and handling of silane, SiXtron Advanced Materials has developed a silane-free polymeric solid or liquid source process and aparatus. This novel source contains silicon, carbon, and hydrogen; therefore, silicon carbon nitride film (SiC_xN_y) with different compositions can be obtained by adjusting source composition during the deposition or by changing the NH_3 flow rate. The new source can be adapted to the existing PECVD production line without any modification. Complete solar cells are fabricated with SiC_xN_y film and compared with the conventional SiN_x coated cells.

Work Summary

GIT has completed the following:

- Chemical, optical, and electrical property analysis
- Solar cell fabrication on 45 − 80 Ω/sq phosphorus emitter
- Light induced degradation measurement
- Low illumination performance of SiC_xN_y coated solar cell

Chemical, optical, and electrical property analysis

GIT has performed SiC_xN_y film analysis:

- XPS (X-ray photoelectron spectroscopy) and Elastic Recoil Detection (ERD) for chemical composition
- Woollam variable angle spectroscopic ellipsometer for optical property
- Sinton's photoconductance tool and surface charge analyzer for electrical property

Solar cell fabrication

- Fabricated 5 or 6 inch industrialized full aluminum BSF solar cells using 1 or 2 Ω-cm boron doped Cz wafers with silane SiN_x or silane-free SiC_xN_y AR coating

Light induced degradation (LID) measurement

- Reduced LID was observed on SiC_xN_y coated solar cells

Low illumination performance of SiC_xN_y coated solar cell

- SiCxNy coated solar cells have extremely high shunt resistance
- Small efficiency degradation on low illumination due to its high shunt resistance

Section 1: Property of SiC_xN_y film

Chemical composition, optical and electrical properties analysis has performed to evaluate the SiC_xN_y film as for antireflection coating and passivation material.

Chemical composition

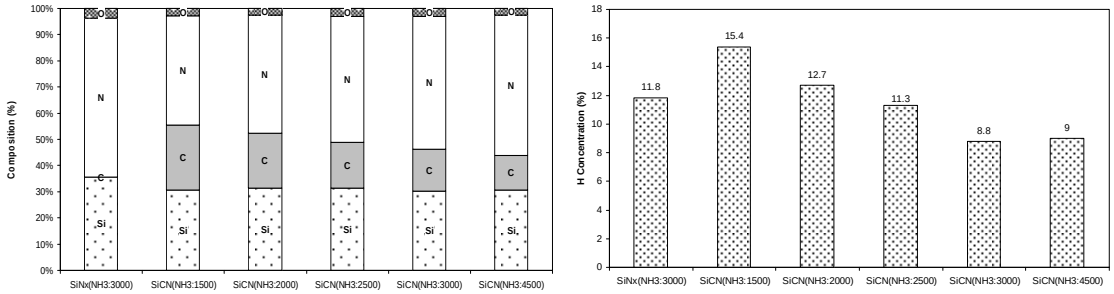

(a) (b)

Figure 1.1. Chemical composition (a) and hydrogen concentration (b) of the dielectric films as a function of NH_3 flow rate. The flow rate of SiH_4 (300sccm) and gas from the solid source (300sccm) was fixed.

Figure 1.1 shows Si/C/N/O chemical composition of SiC_xN_y films and H content as a function of NH_3 gas flow rate during the film deposition. Other deposition parameters including the flow rate of solid polymer gas source (300 sccm), deposition temperature (425 ^oC), pressure (2 Torr), and plasma power (150 W) were fixed for all the depositions in this work. Figure 1.1(a) shows no carbon in the SiN_x film formed with silane gas. However, for films deposited with the new source, nitrogen composition increases in the film with increase in NH_3 gas flow rate while carbon contents decreases. Figure 1.1(b) shows higher hydrogen content in SiN_x films than the SiC_xN_y films deposited with the 3000 sccm ammonia flow rate. In general, the hydrogen composition decreases with increasing NH_3 gas flow rate for the SiC_xN_y films. Note, although the SiN_x films show higher hydrogen content at the same NH_3 flow rate, SiC_xN_y films supply enough hydrogen to passivate defects in the bulk and Si/SiC_xN_y interface during the contact firing. Note, the silicon fraction in the dielectric SiC_xN_y films is constant (around 31%), irrespective of the NH_3 gas flow rate. Thus, by adjusting the NH_3 gas flow rate the carbon composition changes without affecting the silicon composition. Therefore the NH_3 flow rate serves as a tool to adjust the chemical composition of the SiC_xN_y film to approach that of SiN_x formed with SiH_4 gas.

Optical property

Figure 1.2 suggests the refractive index (n) and extinction coefficient (k) decreases with increase in nitrogen content of the SiC_xN_y films. The NH_3 gas flow rate in the range of 1500-4500 sccm was used to obtain similar Si/N composition to that of the SiN_x film. This was tailored to suit our screen printed contact formation process which is optimized for the

conventional SiN_x film. By adjusting the source composition and gas flow rates, SiC_xN_y films with a refractive index in the range of 1.93-2.00 at a wavelength of 630 nm were obtained.

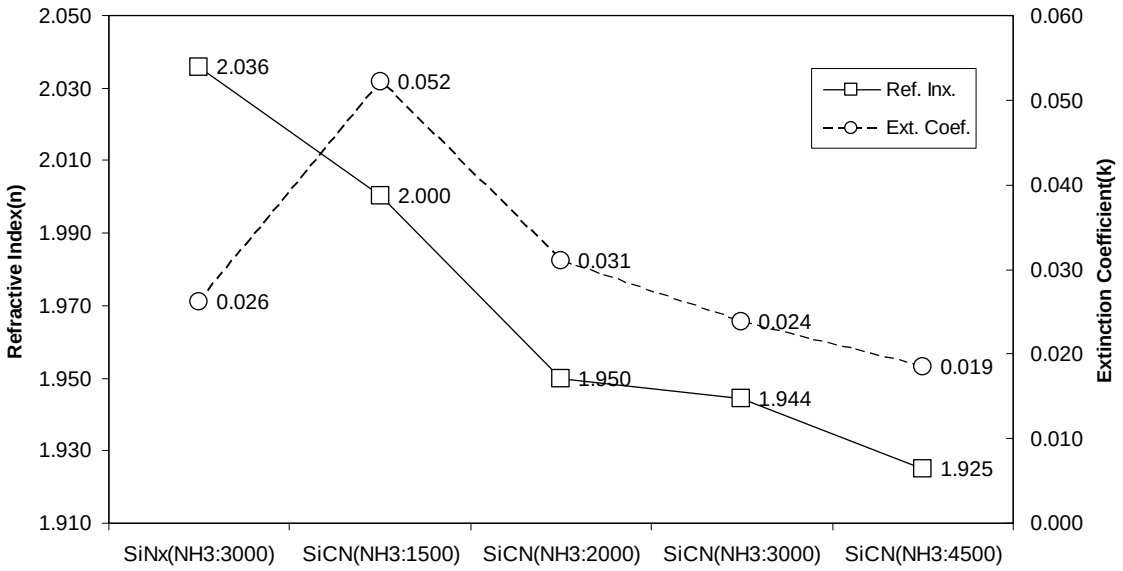

Figure 1.2. Refractive indices (n) and extinction coefficient (k) of the SiN_x and SiC_xN_y films as a function of NH_3 flow rate in sccm. The n and k values were measured at the wavelengths of 630 nm and 300 nm, respectively.

Electrical property

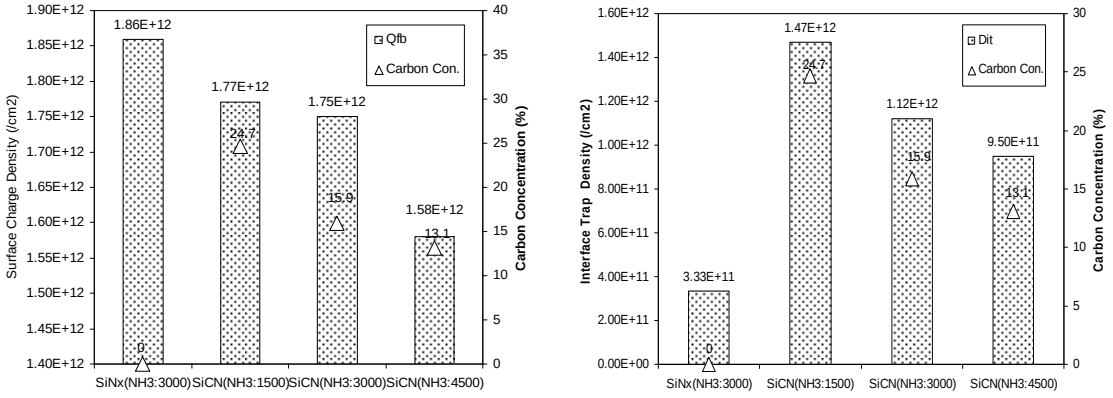

(a) (b)

Figure 1.3. (a)Surface charge densities and carbon concentration and (b) interface trap densities of SiN_x and SiC_xN_y films as a function of NH_3 gas flow rate after annealing in an RTP chamber at 800 ^oC for 2 sec.

Figure 1.3(a) shows the surface charge density, Q_{FB}, in the dielectric films. The surface charge density of dielectrics plays a critical role in controlling the surface passivation and solar cells performance. The positive surface charge density in the SiC_xN_y film was in the range of 1.58-1.77x10^{12}/cm^2 which is high but slightly lower than that of conventional SiN_x film (1.89x10^{12}/cm^2) for these specific samples. However, the surface charge density depends strongly on deposition conditions for SiCxNy such as NH_3 gas flow. Figure 1.3(b) shows the interface trap density (D_{it}) between Si and dielectric film interface. The trap density decreases as carbon contents decreases which suggest that a low carbon concentration is desirable to achieve good surface passivation. However, by increasing the ammonium flow rate to reduce the carbon content increases nitrogen content and decreases the refractive index. This resulted in an optimum NH_3 flow rate of ~ 3000 sccm.

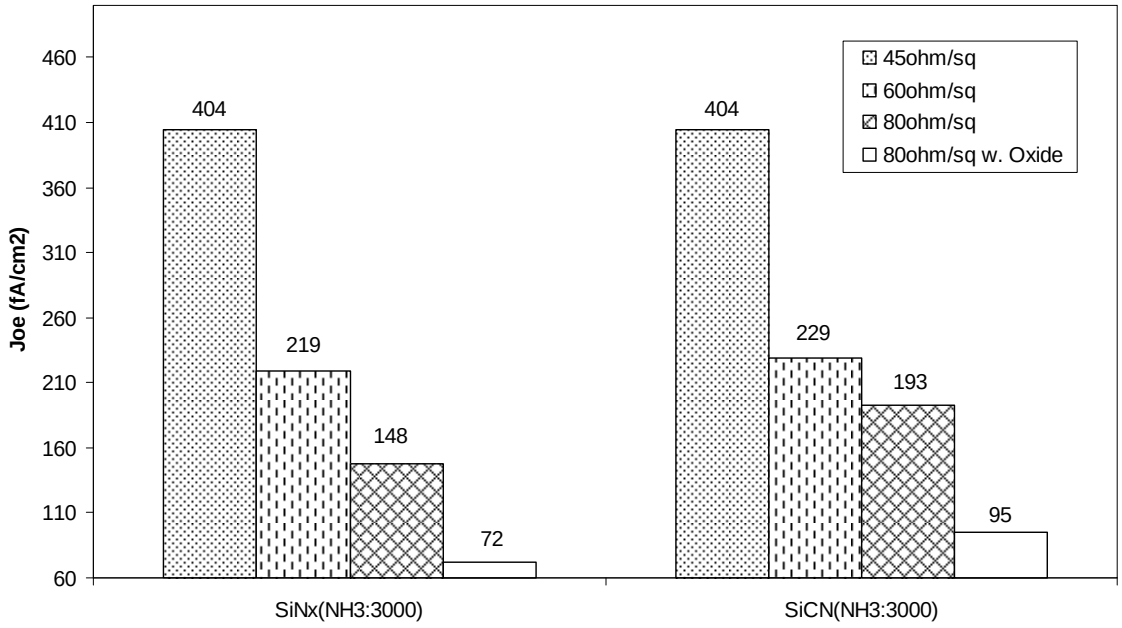

Figure 1.4. J_{oe} values of 45, 60, and 80 ohm/sq emitters at 3000 sccm NH_3 gas flow rate. The samples were annealed in an RTP chamber at 800 ^oC for 2 sec.

Fig 1.4 compares the J_{oe} values for silane deposited SiN_x film and the silane free SiC_xN_y film on 45, 60, and 80 ohm/sq emitters. Both films show similar J_{oe} values for 45 and 60 ohm/sq emitters, but conventional SiN_x showed slightly lower value of J_{oe} than the SiC_xN_y for the 80ohm/sq emitter. This suggests the presence of carbon in the SiC_xN_y films, which may interfere with the hydrogen released from the film to passivate silicon surface. However, with the thermally grown SiO_2 at the interface, the J_{oe} gap decreased for the 80ohm/sq emitter. This suggests the hydrogen released from the film can decrease the interface trap density at the Si/SiO_2 interface.

Conclusion

A novel silane-free solid polymer source was developed at SiXtron Advanced Materials to eliminate the dangerous pyrophoric silane gas in a manufacturing line. The polymer source can be Fedexed, which significantly removes handling and transport issues. Electrical and optical properties of the SiC_xN_y film was studied and compared with that of the conventional SiN_x film formed with pyrophoric SiH_4 as a silicon source. The ratio of carbon to nitrogen (C/N), hydrogen content, refractive index, and extinction coefficient of the SiC_xN_y film was found to decrease with the increase in the NH_3 flow rate. Comparable quality surface passivation of the SiC_xN_y film because of high surface charge density and hydrogen concentration provided low J_{oe} values of ~$4x10^{-13}A/cm^2$ on 45ohm/sq emitter.

Section 2: SiC_xN_y AR coated solar cell fabrication

~2 Ω-cm boron doped Cz silicon wafers were used for substrate material. The as-cut saw damage was removed by a heated potassium hydroxide (KOH) solution. An anisotropic random pyramid texture was applied using a KOH and Isopropyl Alcohol (IPA) mixture. The textured wafers were RCA cleaned followed by 45 - 80 Ω/sq phosphorous emitter diffusion using a standard $POCl_3$ tube furnace diffusion. Following the emitter diffusion, wafers were chemically edge isolated. Same low frequency (50 KHz) PECVD reactor was used for depositing the silane SiN_x and silane-free SiC_xN_y antireflection coating. Front and rear metallization were formed by screen printed silver and aluminum pastes respectively, followed by high temperature belt firing for contact formation and back surface field.

Table 1.1. Performance of 149 cm^2 Cz solar cells with industrial type phosphorus diffused 45, 60, and 80 Ω /sq emitters. NH_3 flow rate was 3000sccm and silane or silane-free source flow rate was 300sccm.

ARC	Plasma Power (W)	V_{oc} (mV)	J_{sc} (mA/cm²)	FF	Eff (%)	Emitter (Ω/sq)
SiN_x	100	624	35.1	0.777	17.0	45
SiC_xN_y	150	622	34.8	0.780	16.9	45
SiNx	100	620	36.1	0.763	17.1	60
SiC_xN_y	150	618	35.8	0.766	17.0	60
SiNx	100	623	36.3	0.767	17.4	80
SiC_xN_y	150	612	36.2	0.775	17.2	80
SiO_2/ SiN_x	100	632	36.2	0.770	17.6	80
SiO_2/ SiC_xN_y	150	625	36.1	0.772	17.4	80

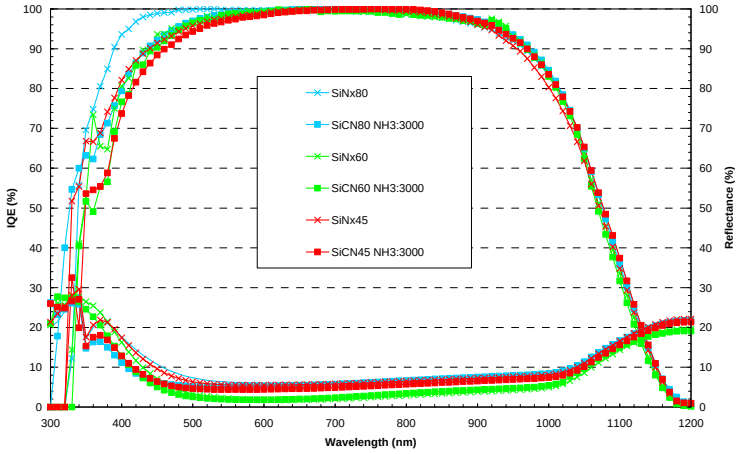

Figure 2.1. IQE responses of the solar cells with the SiN_x AR layer coated using SiH_4 source and SiC_xN_y AR layer coated using the silane-free source with 45, 60, 80 Ω/sq emitters.

Table 1.2. Performance of 149 cm^2 Cz solar cells with industrial type phosphorus diffused 45 Ω /sq emitter as a function of plasma power. NH_3 flow rate was 3000sccm and silane or silane-free source flow rate was 300sccm.

ARC	Plasma Power (W)	Voc (mV)	Jsc (mA/cm^2)	FF	Eff (%)
SiN_x	100	622.9	35.6	0.778	17.2
SiC_xN_y	150	618.0	34.9	0.774	16.7
SiC_xN_y	200	619.3	35.1	0.781	17.0
SiC_xN_y	250	619.4	35.4	0.785	17.2

Table 1.3. Performance of 239 cm^2 Cz solar cells with industrial type phosphorus diffused 60 Ω /sq emitter as a function of plasma power.

ARC	V_{oc} (mV)	J_{sc} (mA/cm^2)	FF	Eff (%)	n factor	Rseries (Ω-cm^2)	Rshunt (Ω -cm^2)
SiN_x	628	37.0	0.783	18.2	1.06	0.697	3296
SiC_xN_y-1	625	36.6	0.787	18.0	1.04	0.680	15348
SiC_xN_y-2	625	36.8	0.786	18.1	1.04	0.687	14536

Conclusion

Screen printed Si solar cells with SiC_xN_y AR coating layer formed from the new silane-free source gave an efficiency of 18.1% on the textured 239cm^2 Cz compared to 18.2% from conventional silane process.

Section 3: LID reduction on SiC_xN_y coated solar cell

There have been some reports of reduced LID in carbon rich Si materials. For example, Schmidt and Bothe reported a 30% reduction in the $B\text{-}O_{2i}$ defects concentration in carbon-contaminated ($C=1.9\text{-}3.3x10^{17}cm^{-3}$) Si material relative to conventional boron doped Si which contains $\sim 5x10^{16}cm^{-3}$ Carbon. In 2006, Coletti et al. also found a reduced concentration of the $B\text{-}O_{2i}$ defects in Si wafers in the presence of carbon. They used multicrystalline (mc) Si wafers with same interstitial oxygen (O_i) concentration (1.5 to $5.6x10^{17}$ cm^{-3}) but different carbon concentrations (2 to 10 ppma). The wafers with a higher carbon concentration (8-10 ppma) showed fewer $B\text{-}O_{2i}$ defects and higher bulk lifetime after LID compared to the wafers with lower (2-4 ppma) carbon concentration. We observed carbon can be incorporated into bulk Si during cell processing via modified AR coating. SiC_xN_y antireflection coating contains significant amount of in situ carbon. Therefore the SiC_xN_y film can serve as a source of carbon during the subsequent high temperature processing. In this experiment, we found that it indeed supplies additional carbon into the bulk during the high temperature annealing or contact firing. Diffused carbon in the bulk competes with boron and effectively reduces the concentration of $B\text{-}O_{2i}$ complex. As a result, SiC_xN_y coated solar cells showed less LID than the solar cells coated with SiN_x film without the in situ carbon.

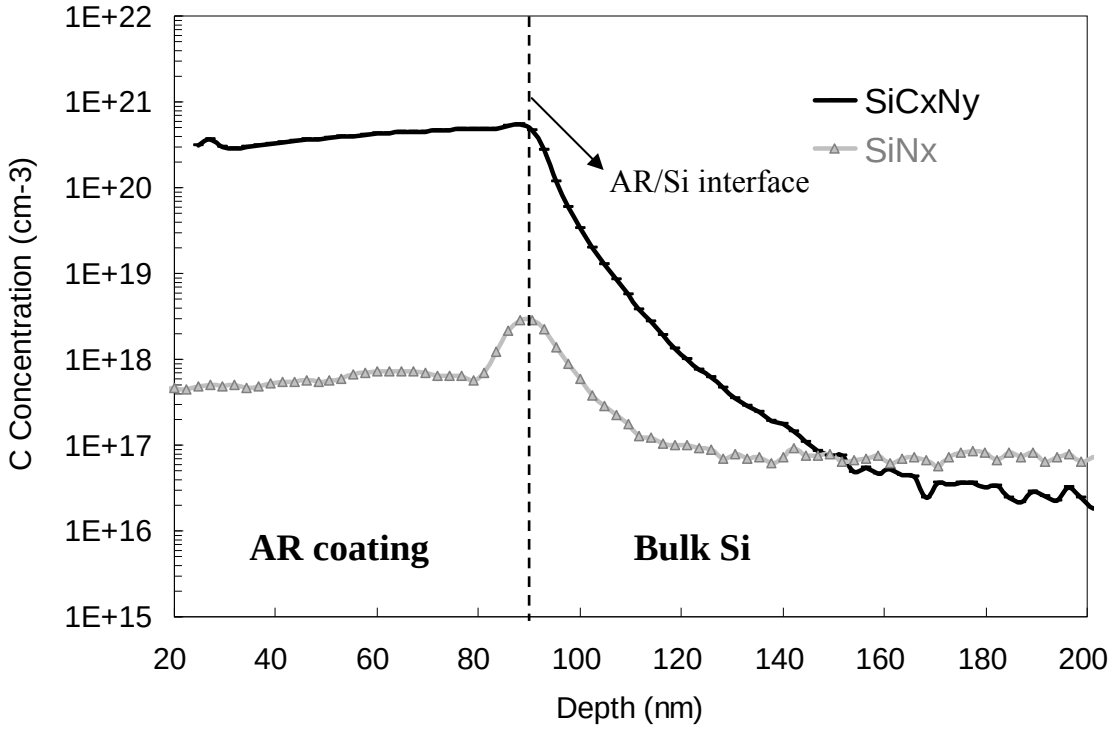

Figure 3.1. SIMS profile of carbon inside the Cz wafers after high temperature annealing. Significant amount of carbon is injected from SiC_xN_y film and diffuses into the bulk Si.

Solar cell results

Large number of SiN_x and $SiCxN_y$ solar cells were fabricated on boron doped Cz wafers to investigate the LID. Figure 3.2 summarizes the statistical degradation of 22 SiN_x and 37 SiC_xN_y coated boron doped Cz (oxygen ~$7x10^{17}cm^{-3}$) solar cells after ~72hours of illuminations. It is clear from Figure 3.2 that SiC_xN_y coated solar cells show lower LID than SiN_x coated cells. $SiCxN_y$ coated solar cells showed an average loss of 0.1% in absolute efficiency compared to 0.3% loss in efficiency for the SiN_x coated cells. In addition, LID-induced loss in V_{oc} and J_{sc} of the SiN_x coated cells was approximately twice that of the $SiCxN_y$ coated cells. Quantitatively 59% of SiN_x coated solar cells suffered a loss of 0.3 - 0.6% in absolute efficiency after the LID while 75% SiC_xN_y coated solar cells showed a LID of ≤0.1% along with 32% cells with no LID. It is interesting to note that this nearly makes up for the ~0.2% lower initial efficiency of the SiC_xN_y coated cells, compared to SiN_x coated cells, due to a slightly inferior surface passivation. Consequently SiN_x and SiC_xN_y coated cells in this study showed nearly the same efficiency after the LID.

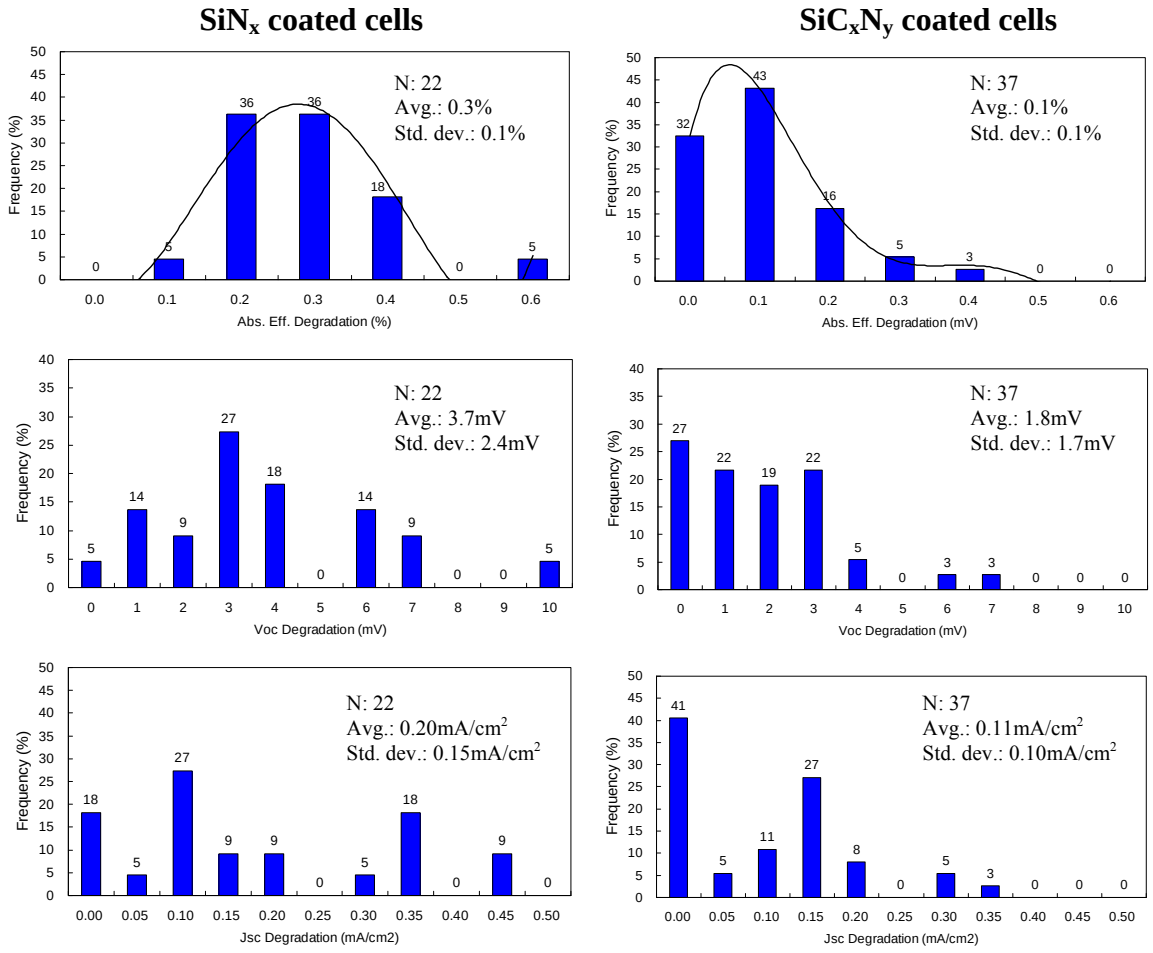

Figure 3.2. Statistical plot of degradation after several hours of illumination of boron doped Cz solar cells with SiN_x (left) or SiC_xN_y (Right) AR coating.

PC1D simulation

In order to quantify and understand the LID phenomena in both kinds of cells, we measured internal quantum efficiency (IQE) and bulk lifetime in the finished cells, before and after LID. By matching the measured and modeled short and long wavelength response, using the measured bulk lifetime value, we extracted the front and back surface recombination velocities (FSRV and BSRV). We found that LID has no effect on the FSRV and BSRV values. However, FSRV value was lower in the case of SiN_x AR coating (45,000cm/s as opposed to 75,000cm/s) which accounts for the ~0.2% higher pre-LID efficiency of the SiN_x coated cells. Figure 3.3 shows that the LID lowered the bulk lifetime from 234 to 113us in the SiN_x coated cells which, according to PC1D model calculations, accounts for the observed ~0.2% loss in efficiency from 17.3% to 17.1%. In the case of SiC_xN_y coated cells lifetime decreased from 250 to 160us after LID which amounts to a negligible loss in efficiency because efficiency becomes insensitive to bulk lifetime above 150us for the current cell design. This is supported by the PC1D model calculations shown in Figure 3.4. Therefore the cell efficiency remains ~17.1% before and after LID in the SiC_xN_y coated cells, which is quite comparable to the SiN_x coated cells after the LID.

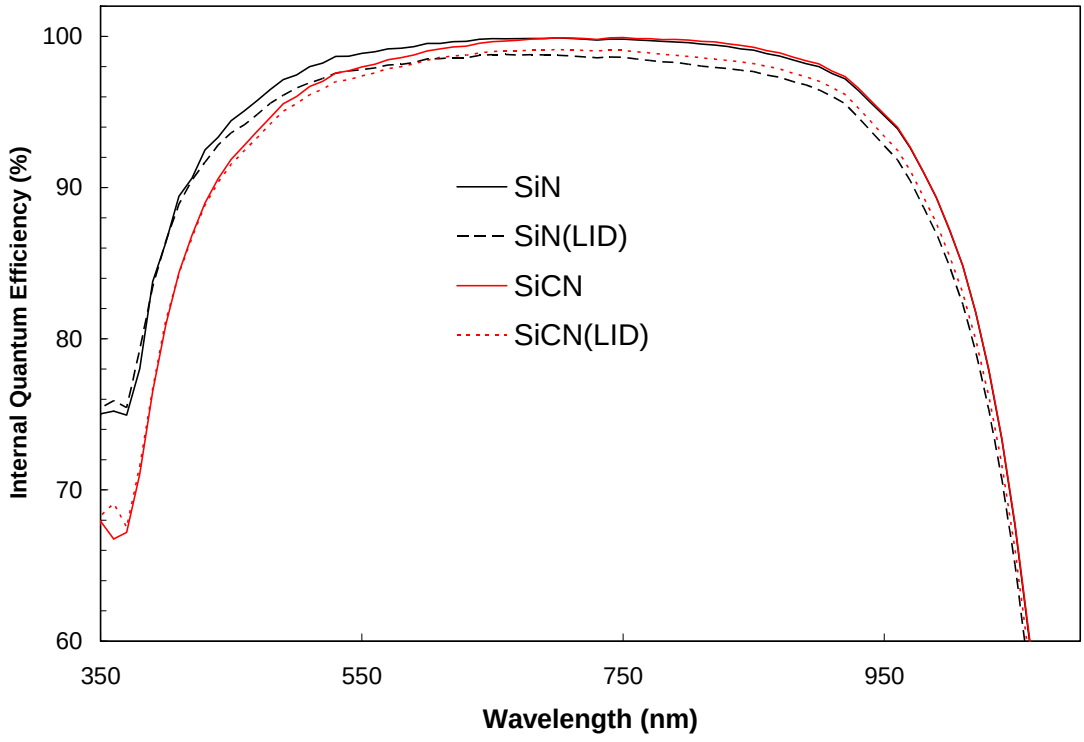

(a)

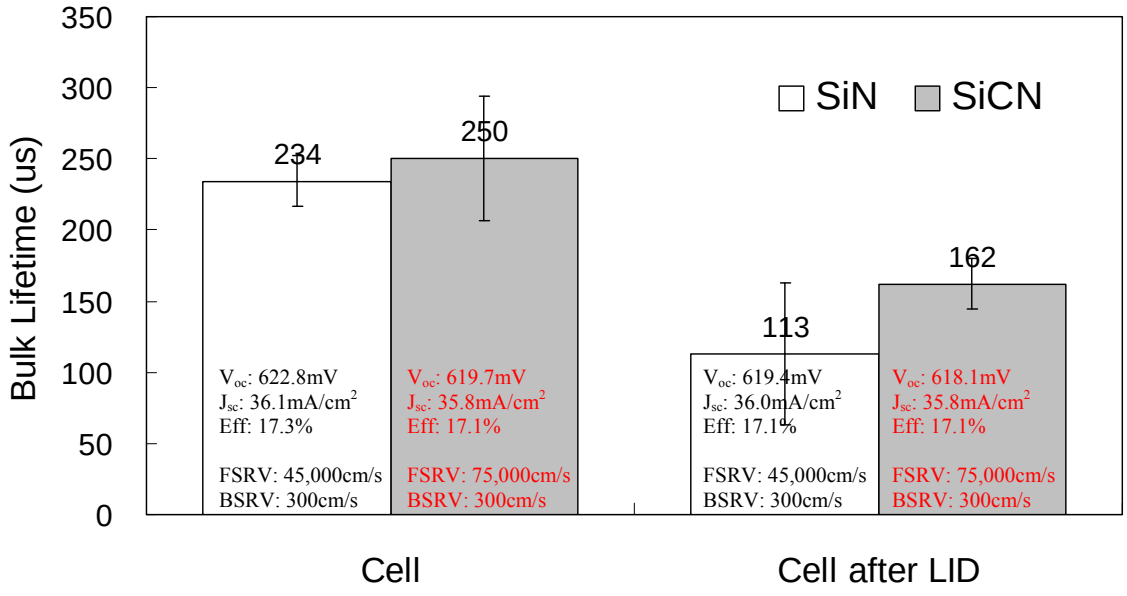

(b)

Figure 3.3. Internal quantum efficiency (IQE) (a) and bulk lifetime and corresponding solar cell values (b) from PC1D for SiN_x and SiC_xN_y coated solar cell.

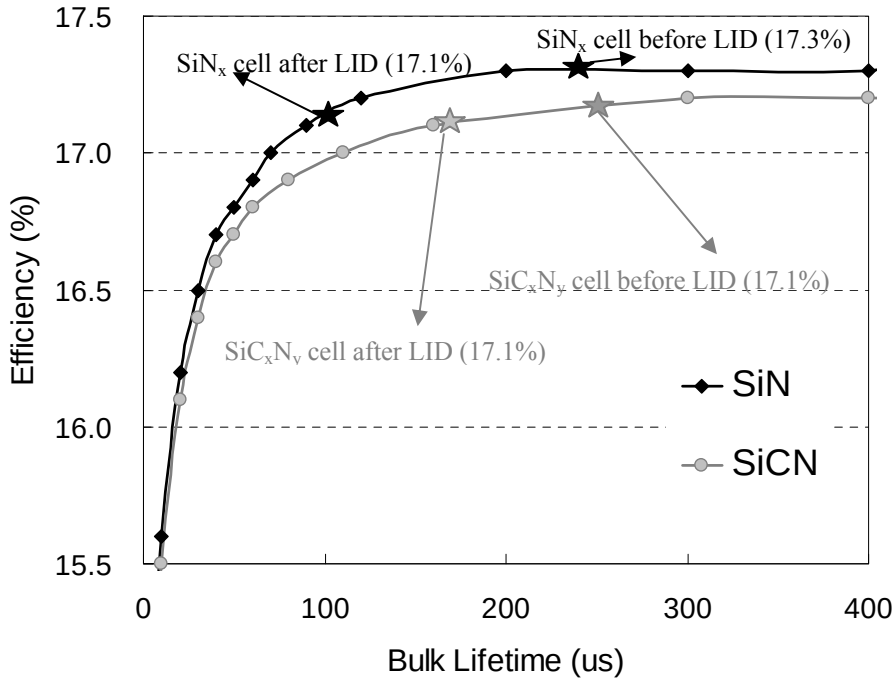

Figure 3.4. Solar cell efficiency as a function of bulk lifetime.

Conclusion

Carbon inside the SiC_xN_y AR coating diffuses into Si after the deposition and high temperature contact firing and competes with boron to form complex with oxygen dimmers. This reduces the number of B-O_{2i} metastable defect complexes which are responsible for LID. As a result, SiC_xN_y coated boron doped Cz solar cells show appreciably less LID compared to conventional SiN_x coated solar cells, which have no source of additional carbon. In this study SiN_x coated solar cells suffered an average loss of 0.3% in absolute efficiency due to LID compared to 0.1% for the SiC_xN_y coated solar cells. PC1D simulations showed that the observed efficiency loss is entirely consistent with the measured bulk lifetime degradation from 234 to 113us and 250 to 160us in the SiN_x and SiC_xN_y coated cells, respectively. This is because efficiency is very weak function of bulk lifetime in the range of 160 to 250us.

Section 4: Low illumination performance of SiC_xN_y coated solar cell

We have studied the beneficial effect of carbon containing AR coating on screen-printed metal contact formation and the cell performance under low illumination. It is well known that if the shunt resistance of solar cell is more than (>7 Ω), it does not hurt the cell performance under STC condition (AM 1.5G with intensity of 1000 W/m^2). However, module under operation is seldom under STC condition. Most of the day module is well below the STC condition depending on the geographical location and the weather. Moreover solar cell efficiency decreases at lower than STC illumination due to lower R_{sh} even if the starting cell efficiency is identical. This section shows that SiC_xN_y film deposited by a silane-free organic source gives much higher R_{sh}, which in turns leads to smaller FF degradation, lower efficiency loss, and higher annual energy production. Theoretical calculations are performed first to calculate the effect of R_{sh} on FF and efficiency as a function of illumination level.

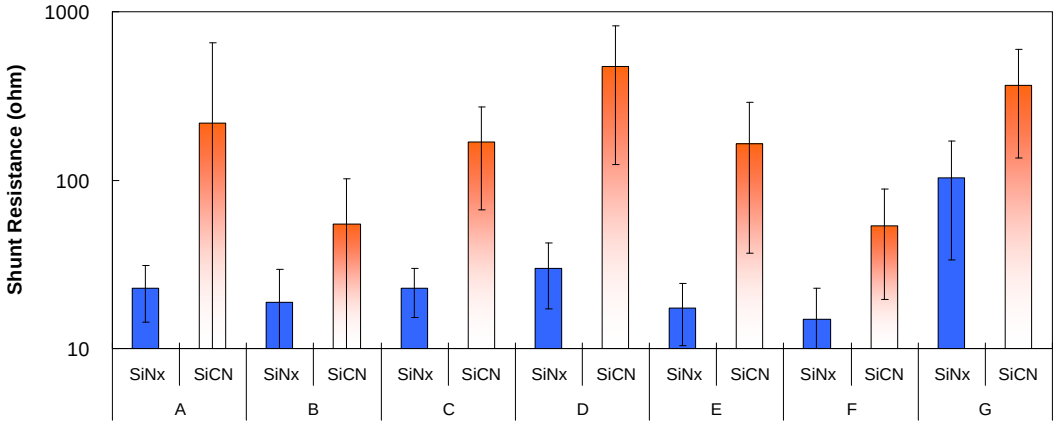

(a)

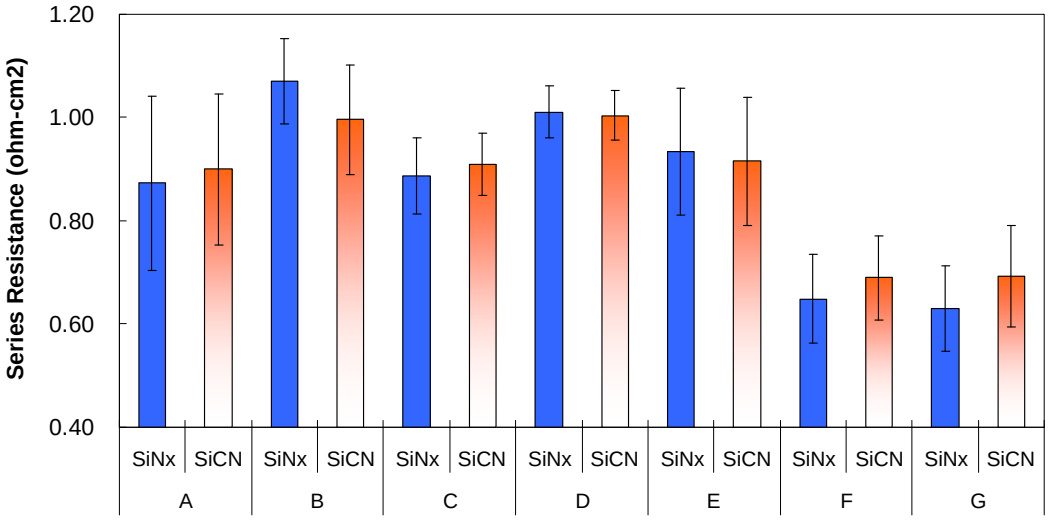

(b)

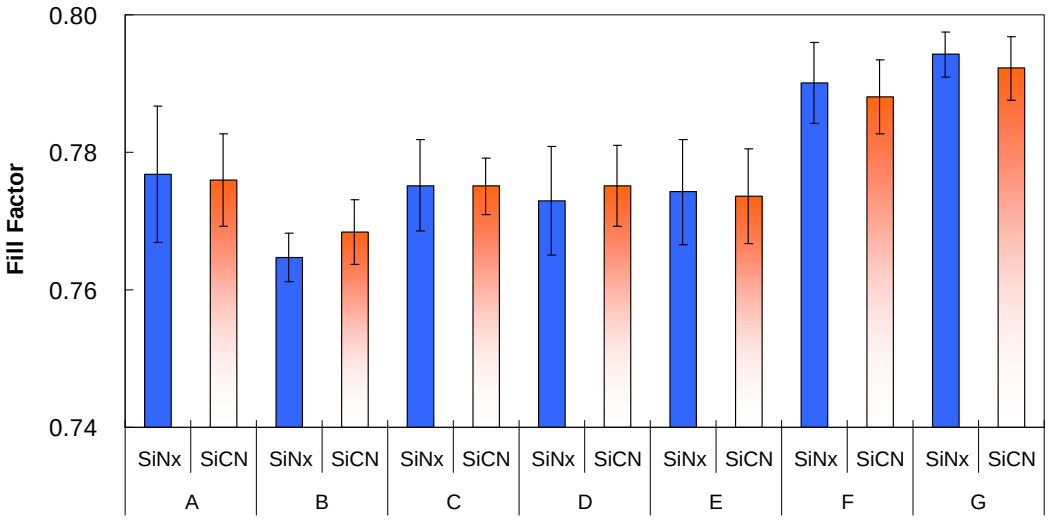

(c)

Figure 4.1. Average values of (a) Shunt resistance, (b) series resistance, and (c) Fill factor from several hundred SiN_x and SiC_xN_y coated solar cells fabricated with different silver pastes.

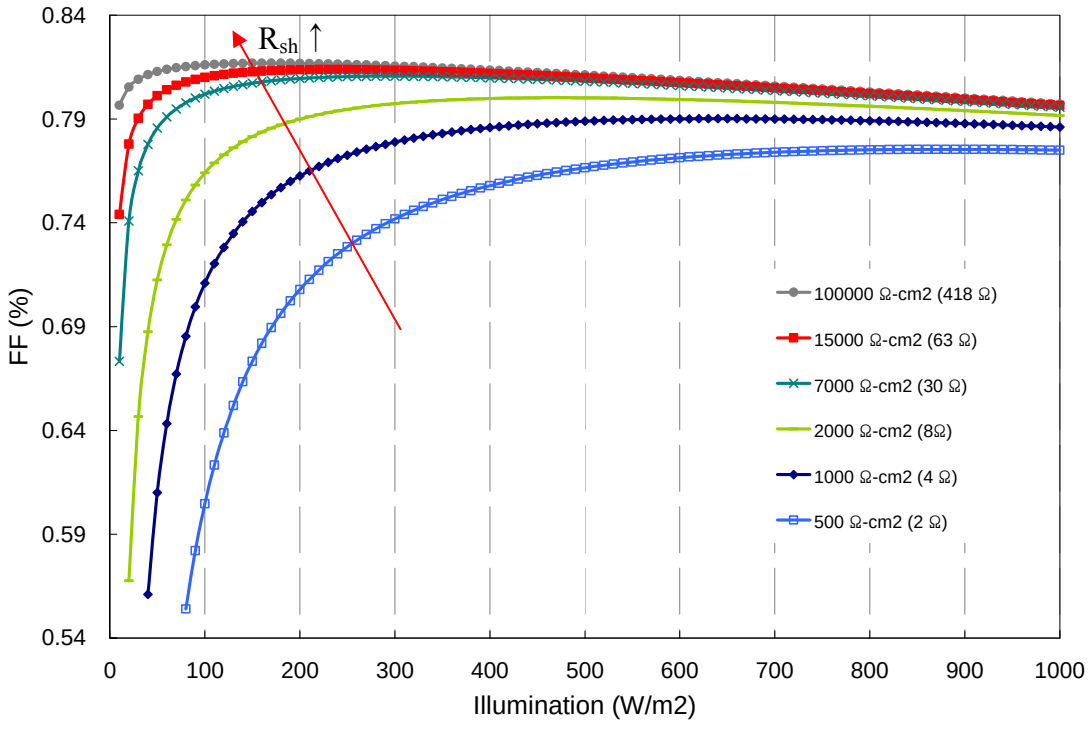

(a)

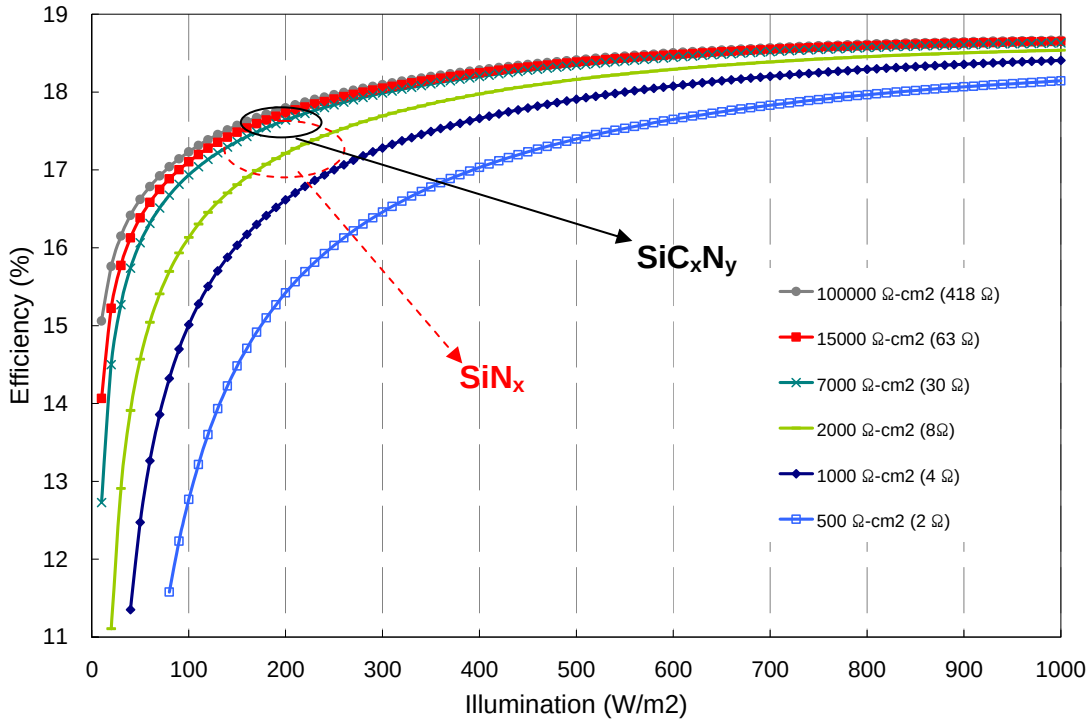

(b)

Figure 4.2. (a) Calculated FF and (b) solar cell efficiency (Area = 239cm^2, V_{oc} = 630 mV, and J_{sc} = 37mA/cm^2 at STC) as a function of illumination intensity with various shunt resistance. Based on measured statistical shunt resistance data, range of SiN_x and SiC_xN_y solar cells are marked on the Figure.

In order to validate the model calculations in Figure 4.2, we also measured the SiN_x and SiC_xN_y coated solar cell efficiency, with known value of R_{sh}, at various illuminations. Experimental data agrees fairly well with the model calculations (Figure 4.3). Also note that even though SiN_x cell efficiency was slightly higher (~0.2%) at 1 Sun, the SiC_xN_y cell efficiency became equal or greater than the SiN_x coated cells at below 600 W/m^2 illuminations even though its starting efficiency at 1 Suns was ~0.2% lower.

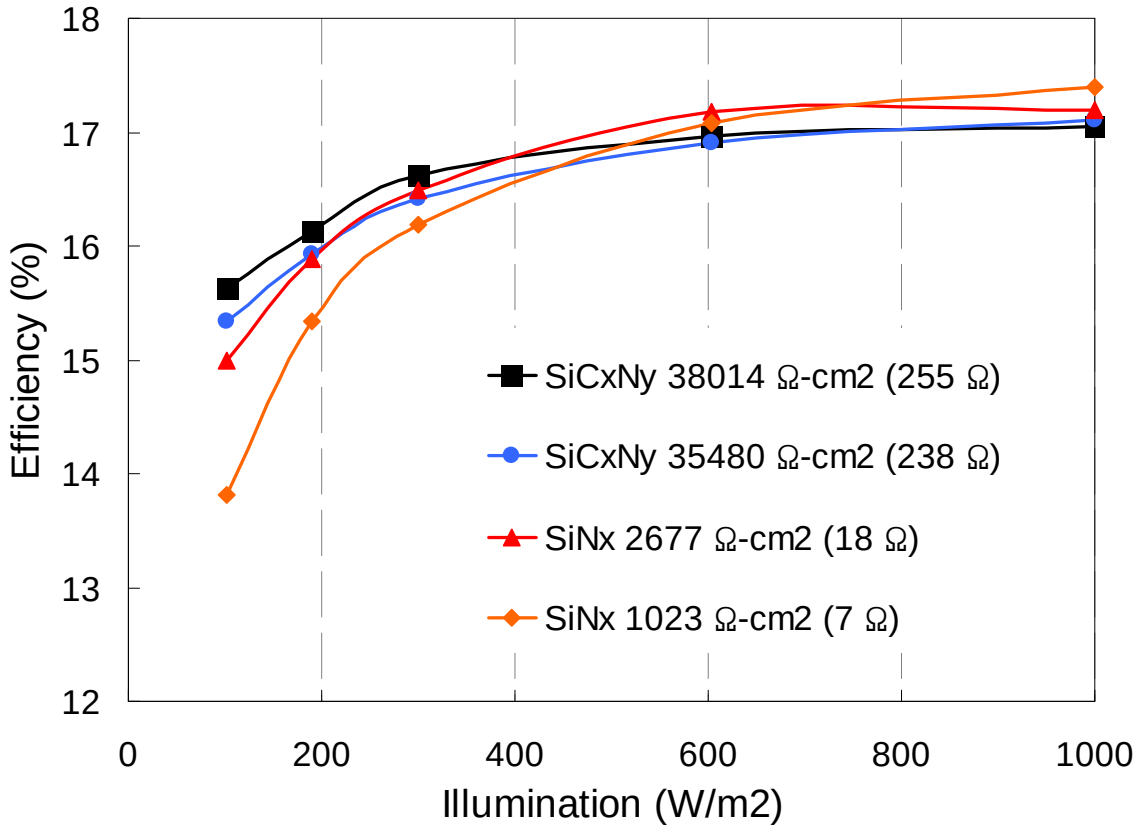

Figure 4.3. Measured solar cell efficiency as a function of illumination intensity of SiN_x and SiC_xN_y coated solar cells. Values for SiC_xN_y coated solar cells are gray-highlighted.

SAM program from NREL was used to quantify the effect of R_{sh} on annual energy production and LCOE for locations with various solar insolation (high, medium, and low). Recently released SAM (Version 2010.11.9) has the capability to account for the impact of change in efficiency as a function of solar irradiance. Efficiency Vs. insolation data in Figure 4.2 was fed into the SAM model for different R_{sh} values. Other key inputs for SAM are shown in Table 4.1. SAM's output includes annual energy production and LCOE. Four different locations, Phoenix, LA, Atlanta, and Seattle, were selected for comparison because they have appreciably different solar insolation ranging from 2117 KWh/m^2-yr to 1222 KWh/m^2-yr. Figure 4.4 shows the change in calculated annual energy production and LCOE as a function of location and R_{sh} value. It is found that for any given location if the R_{sh} is above 30 Ω or 7000 Ω-cm^2, then R_{sh} has very little affect on LCOE. However if R_{sh} is below 15 Ω or 3000 Ω-cm^2, it could reduce the energy production and raise the LCOE. In addition, the impact of R_{sh} below 15 Ω is increased for regions of lower solar insolation like Seattle. Because SiC_xN_y coated solar cells show always high shunt resistance (>30 Ω) compared to SiN_x, its slightly lower initial efficiency (~0.1 - 0.2%) at STC is compensated by higher R_{sh} with regards to annual energy production.

Table 4.1. Specified parameters used for SAM calculation. Values are referenced from DOE MYPP Benchmarks for residential.

System element	
Module efficiency at STC (%)	16.0
Number of module	40
PV module cost ($/W)	1.82
Inverter cost ($/W)	0.69
BOS cost ($/W)	0.40
Installation cost ($/W)	0.57
Indirect cost ($/W)	1.14
Inverter efficiency (%)	90
System loss (%)	10.5
Annual fixed O&M	0.5% of installed system cost

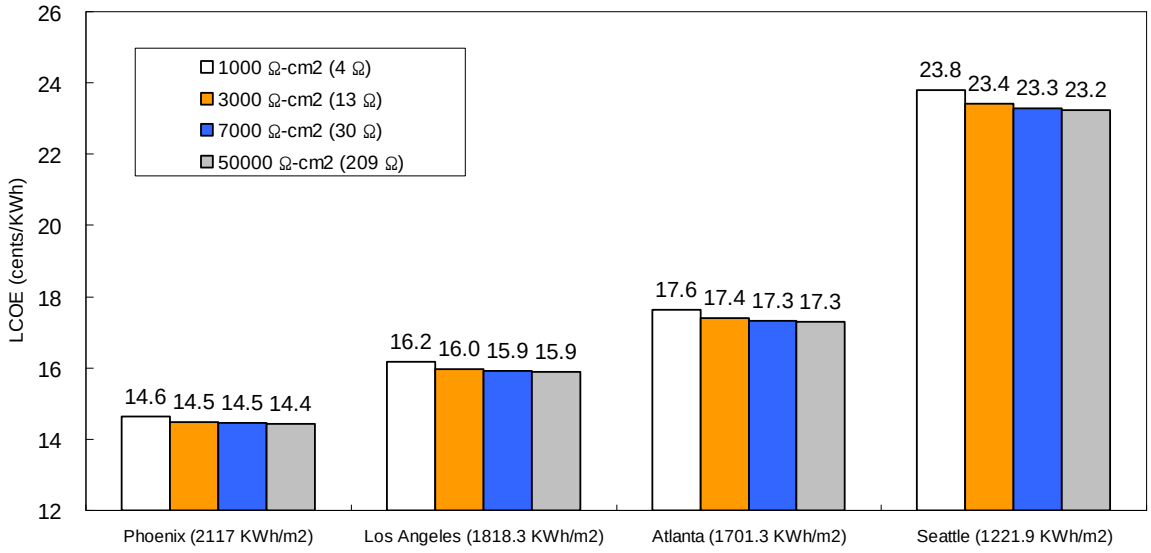

(a)

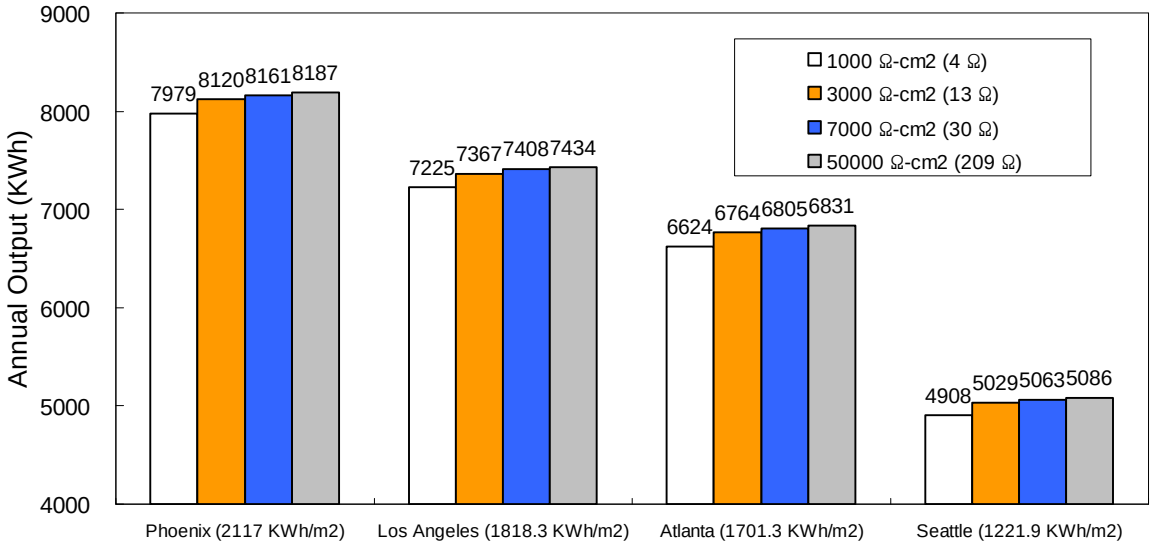

(b)

Figure 4.4. (a) LCOE and (b) annual power output calculation using SAM with various illumination regions and shunt resistances.

Conclusion

It is found that carbon containing SiC_xN_y film show much higher R_{sh} value after contact firing compared to its counterpart carbon free SiN_x film. The size of silver crystallites at the contact interface are smaller in the presence of carbon in the AR coating which reduces the parasitic shunting in the cell. Theoretical calculations and experimental data confirm that lower R_{sh} values reduce the cell efficiency at lower insolation. Economic calculations show that shunt resistance above 30 Ω or 7000 Ω-cm^2 is required to minimize the loss in energy production or increase in LCOE due to R_{sh} induced loss in efficiency at reduced illumination. Shunt resistance of SiC_xN_y cell was mostly over 60 Ω compared to the SiN_x coated cells, which average around 23 Ω 5500 Ω-cm^2. This makes up for slightly lower starting efficiency of SiC_xN_y coated cells compared to SiN_x coated cells.